Hadronic contributions to $g-2$ of the muon — theory —

Bastian Kubis

HISKP (Theorie) & BCTP

Universität Bonn, Germany

20/5/2021

MESON 2021

Outline

The anomalous magnetic moment of the muon

Hadronic vacuum polarisation

- The $\pi^+\pi^-\pi^0$ channel — Hoferichter, Hoid, BK, JHEP **1908** (2019) 137
- The $\pi^0\gamma$ channel — Hoid, Hoferichter, BK, Eur. Phys. J. **80** (2020) 988

Hadronic light-by-light scattering

- Dispersive analysis of the π^0 transition form factor
- High-energy asymptotics — Hoferichter, Hoid, BK, Leupold, Schneider, Phys. Rev. Lett. **121** (2018) 112002; JHEP **1810** (2018) 141
- Putting pieces together — Aoyama et al., Phys. Rept. **887** (2020) 1

Summary / Outlook

The anomalous magnetic moment of the muon

- gyromagnetic ratio: magnetic moment $\leftrightarrow$ spin

$$\vec{\mu} = g\frac{e}{2m}\vec{S} \qquad \text{Dirac:} \quad g_\mu = 2$$

- rad. corr.: $g_\mu = 2(1 + a_\mu)$, $\quad a_\mu$ "anomalous magnetic moment"
- one of the most precisely measured quantities in particle physics

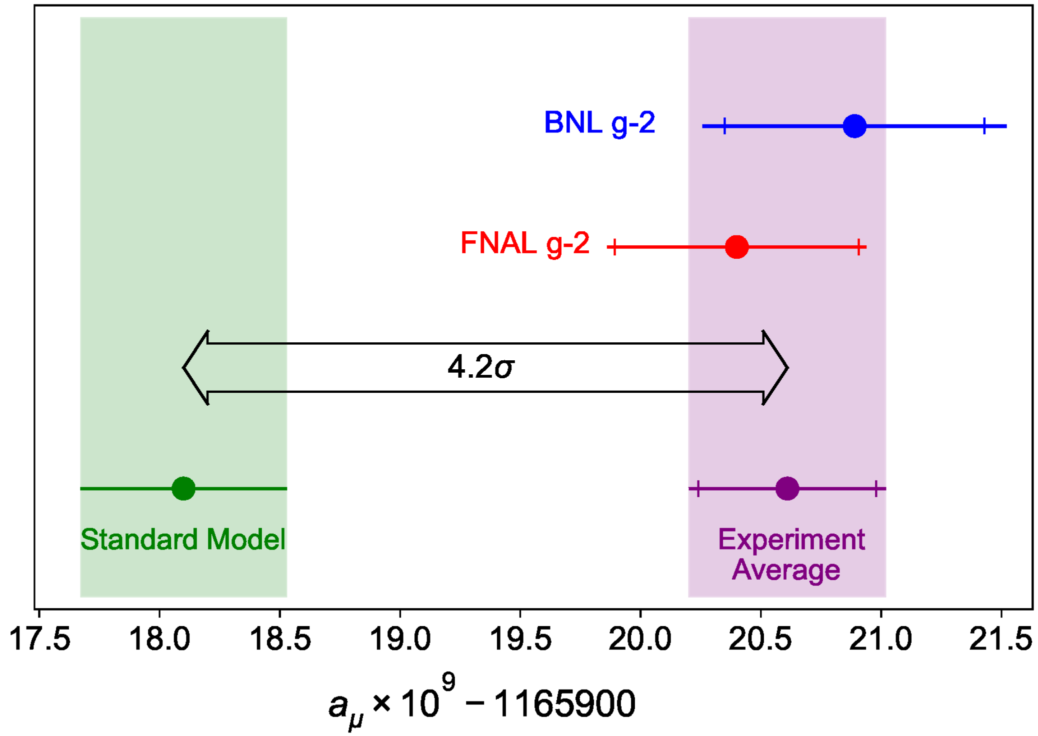

$\longrightarrow 4.2\sigma$ discrepancy: $\qquad a_\mu^{\text{exp}} - a_\mu^{\text{SM}} = (251 \pm 59) \times 10^{-11}$

BNL E821 2006, Fermilab 2021; Aoyama et al. 2020

Hadronic contributions to a_μ

	$a_\mu\ [10^{-11}]$	$\Delta a_\mu\ [10^{-11}]$
experiment	116 592 061.	41.
QED $\mathcal{O}(\alpha)$	116 140 973.321	0.023
QED $\mathcal{O}(\alpha^2)$	413 217.626	0.007
QED $\mathcal{O}(\alpha^3)$	30 141.902	0.000
QED $\mathcal{O}(\alpha^4)$	381.004	0.017
QED $\mathcal{O}(\alpha^5)$	5.078	0.006
QED total	116 584 718.931	0.030
electroweak	153.6	1.0
had. VP (LO)	6931.	40.
had. VP (NLO)	–98.3	0.7
had. LbL	92.	19.
total	116 591 810.	43.

BNL E821 2006
+ Fermilab 2021

Aoyama et al. 2020

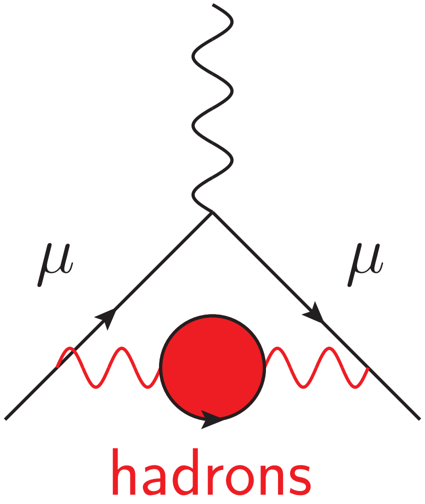

Hadronic contributions to a_μ

	$a_\mu\ [10^{-11}]$	$\Delta a_\mu\ [10^{-11}]$
experiment	116 592 061.	41.
QED $\mathcal{O}(\alpha)$	116 140 973.321	0.023
QED $\mathcal{O}(\alpha^2)$	413 217.626	0.007
QED $\mathcal{O}(\alpha^3)$	30 141.902	0.000
QED $\mathcal{O}(\alpha^4)$	381.004	0.017
QED $\mathcal{O}(\alpha^5)$	5.078	0.006
QED total	116 584 718.931	0.030
electroweak	153.6	1.0
had. VP (LO)	6931.	40.
had. VP (NLO)	–98.3	0.7
had. LbL	92.	19.
total	116 591 810.	43.

BNL E821 2006
+ Fermilab 2021

Aoyama et al. 2020

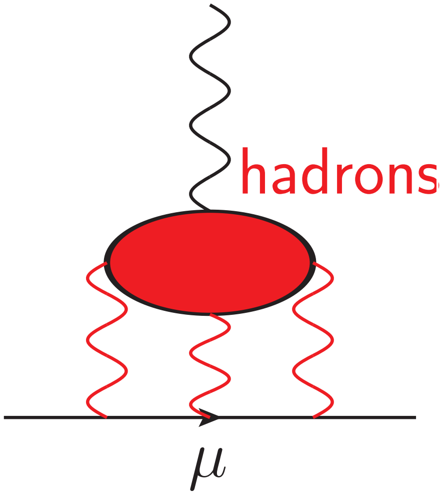

Hadronic vacuum polarisation

- how to control hadronic vacuum polarisation?
- characteristic scale set by muon mass
  $\longrightarrow$ this is not a perturbative QCD problem!
- dispersion relations to the rescue:
  use the optical theorem!

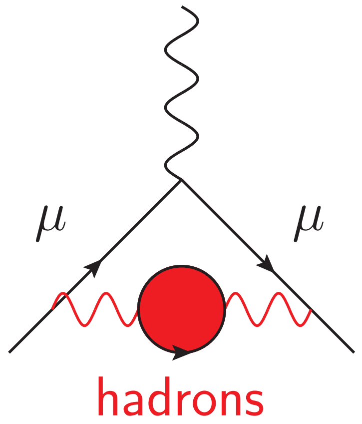

Im 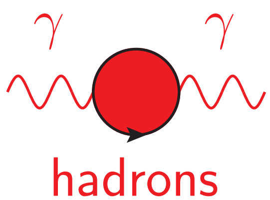

$\Leftrightarrow$ $\Bigg|$ 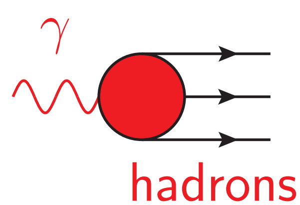

$\Bigg|^2$ $\propto \sigma_{\text{tot}}(e^+e^- \to \text{hadrons})$

Hadronic vacuum polarisation

- how to control hadronic vacuum polarisation?
- characteristic scale set by muon mass
  $\longrightarrow$ this is not a perturbative QCD problem!
- dispersion relations to the rescue:
  use the optical theorem!

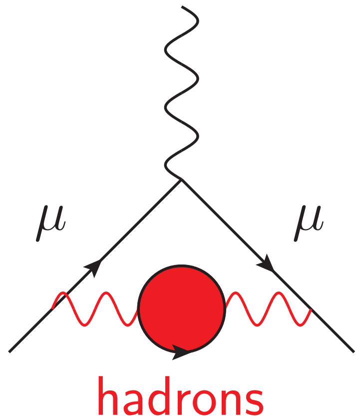

$$a_\mu^{\text{had VP}} \propto \int_{4M_\pi^2}^{\infty} ds\, K(s)\sigma_{\text{tot}}(e^+e^- \to \text{hadrons})$$

- $K(s)$: kinematical function, for large s: $\quad K(s) \propto 1/s$,
  $\sigma_{\text{tot}}(e^+e^- \to \text{hadrons}) \propto 1/s$

- more than 75% of $a_\mu^{\text{had VP}}$ given by
  energies $s \leq 1\,\text{GeV}^2$ Jegerlehner, Nyffeler 2009
- well constrained by data

BABAR, BESIII, CMD, KLOE, SND, ...

$\longrightarrow$ see talk by A. Denig

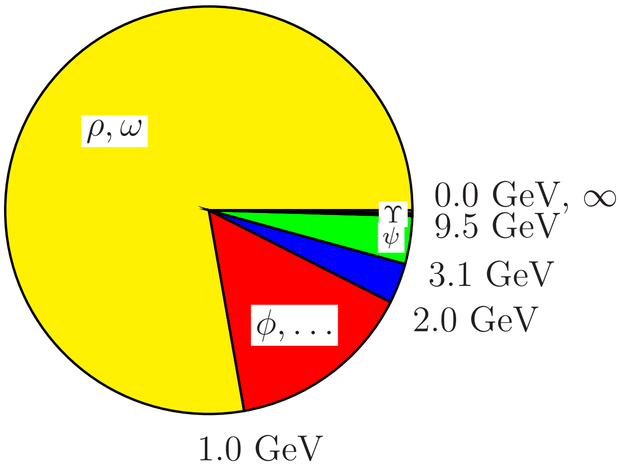

Hadronic light-by-light scattering

- hadronic light-by-light:
  - ▷ subleading in α_{QED}
  - ▷ large relative uncertainty

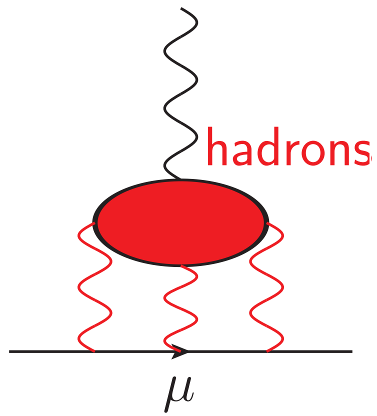

- different contributions calculated or estimated (in 10^{-11}):

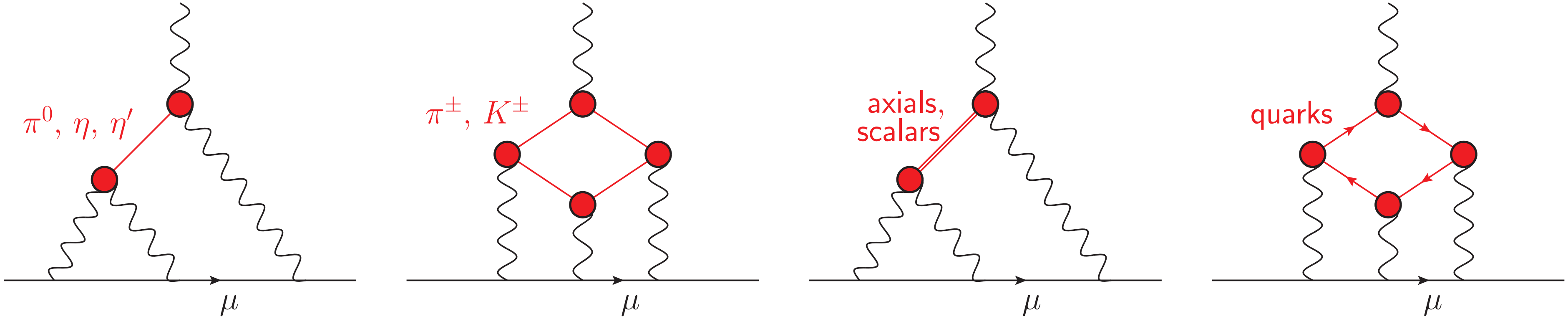

94±4   –24±1   5±7   18±10

$\longrightarrow$ increasing systematic control over HLbL using
dispersion-theoretical approach

Aoyama et al. 2020

Hadronic light-by-light: dispersive approach

Colangelo, Hoferichter, Procura, Stoffer 2014, 2015

- HLbL tensor $\Pi^{\mu\nu\lambda\sigma}$: Lorentz invariance

  $\longrightarrow$ 138 (136) scalar functions Eichmann et al. 2014

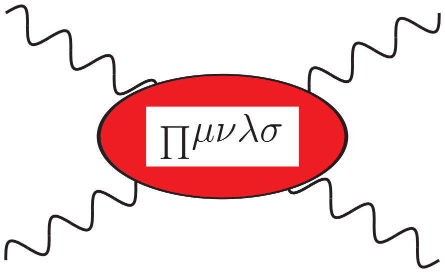

- gauge invariance: Bardeen, Tung 1968; Tarrach 1975

$$\Pi^{\mu\nu\lambda\sigma} = \sum_{i=1}^{54} T_i^{\mu\nu\lambda\sigma}\Pi_i$$

$\longrightarrow$ 7 distinct structures, 47 related by crossing

Hadronic light-by-light: dispersive approach

Colangelo, Hoferichter, Procura, Stoffer 2014, 2015

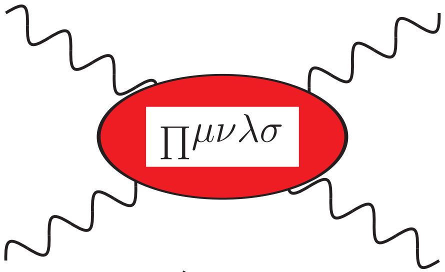

- HLbL tensor $\Pi^{\mu\nu\lambda\sigma}$: Lorentz invariance

  $\longrightarrow$ 138 (136) scalar functions Eichmann et al. 2014
- gauge invariance: Bardeen, Tung 1968; Tarrach 1975

$$\Pi^{\mu\nu\lambda\sigma} = \sum_{i=1}^{54} T_i^{\mu\nu\lambda\sigma} \Pi_i$$

  $\longrightarrow$ 7 distinct structures, 47 related by crossing

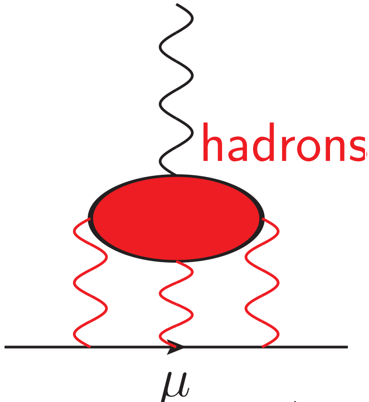

- master formula:

$$a_\mu^{\text{HLbL}} = -e^6 \int \frac{d^4 q_1}{(2\pi)^4} \frac{d^4 q_2}{(2\pi)^4} \frac{\sum_{i=1}^{12} \hat{T}_i(q_1, q_2; p) \hat{\Pi}_i(q_1, q_2, -q_1 - q_2)}{q_1^2 q_2^2 (q_1 + q_2)^2 [(p + q_1)^2 - m_\mu^2][(p - q_2)^2 - m_\mu^2]}$$

- $\hat{T}_i$: known kernels

  $\hat{\Pi}_i$: dispersively $\leftrightarrow$ measurable form factors / scatt. amplitudes

Hadronic light-by-light: dispersive approach

Colangelo, Hoferichter, Procura, Stoffer 2014, 2015

- HLbL tensor $\Pi^{\mu\nu\lambda\sigma}$: Lorentz invariance
  $\longrightarrow$ 138 (136) scalar functions Eichmann et al. 2014

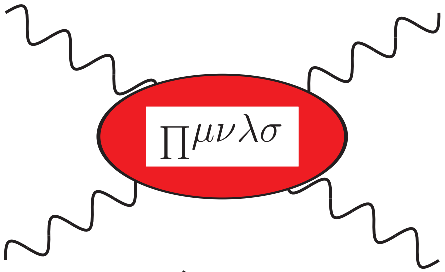

- gauge invariance: Bardeen, Tung 1968; Tarrach 1975

$$\Pi^{\mu\nu\lambda\sigma} = \sum_{i=1}^{54} T_i^{\mu\nu\lambda\sigma} \Pi_i$$

$\longrightarrow$ 7 distinct structures, 47 related by crossing

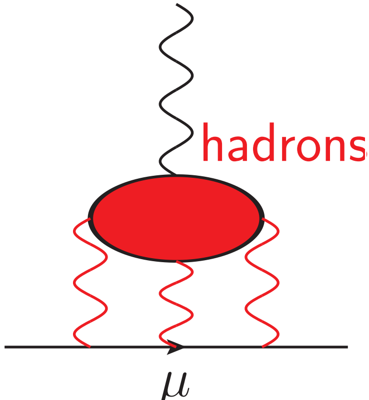

- master formula:

$$a_\mu^{\mathrm{HLbL}} = -e^6 \int \frac{d^4 q_1}{(2\pi)^4} \frac{d^4 q_2}{(2\pi)^4} \frac{\sum_{i=1}^{12} \hat{T}_i(q_1, q_2; p) \hat{\Pi}_i(q_1, q_2, -q_1 - q_2)}{q_1^2 q_2^2 (q_1 + q_2)^2 [(p + q_1)^2 - m_\mu^2][(p - q_2)^2 - m_\mu^2]}$$

- $\hat{T}_i$: known kernels
  $\hat{\Pi}_i$: dispersively $\leftrightarrow$ measurable form factors / scatt. amplitudes
- alternative approaches: disp. rel. for F_2 Pauk, Vanderhaeghen 2014
  Schwinger sum rule Hagelstein, Pascalutsa 2017

Hadronic light-by-light: the π^0 pole

- largest individual HLbL contribution:

  π^0 pole term

  singly / doubly virtual transition
  form factors (TFFs)

  $F_{\pi^0\gamma^*\gamma^*}(q^2,0)$ and $F_{\pi^0\gamma^*\gamma^*}(q_1^2,q_2^2)$

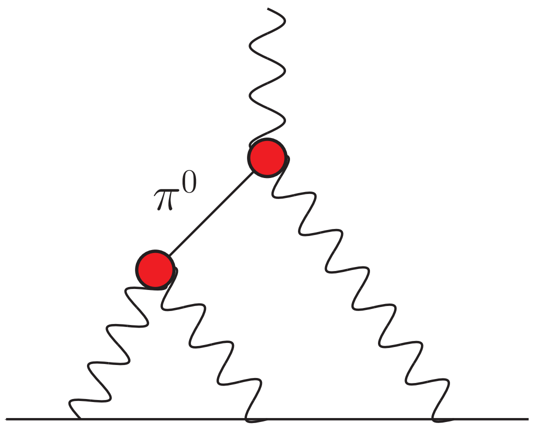

- normalisation fixed by Wess–Zumino–Witten (WZW) anomaly:

$$F_{\pi^0\gamma^*\gamma^*}(0,0) = \frac{1}{4\pi^2 F_\pi}$$

  $\longrightarrow$ measured at 0.75% (F_π: pion decay constant) PrimEx 2020

- two-loop integral with constant form factors does not converge

  $\longrightarrow$ no full prediction from e.g. chiral perturbation theory

  $\longrightarrow$ sensible high-energy behaviour required!

Pion-pole contribution to a_μ

- 3-dimensional integral representation: Jegerlehner, Nyffeler 2009

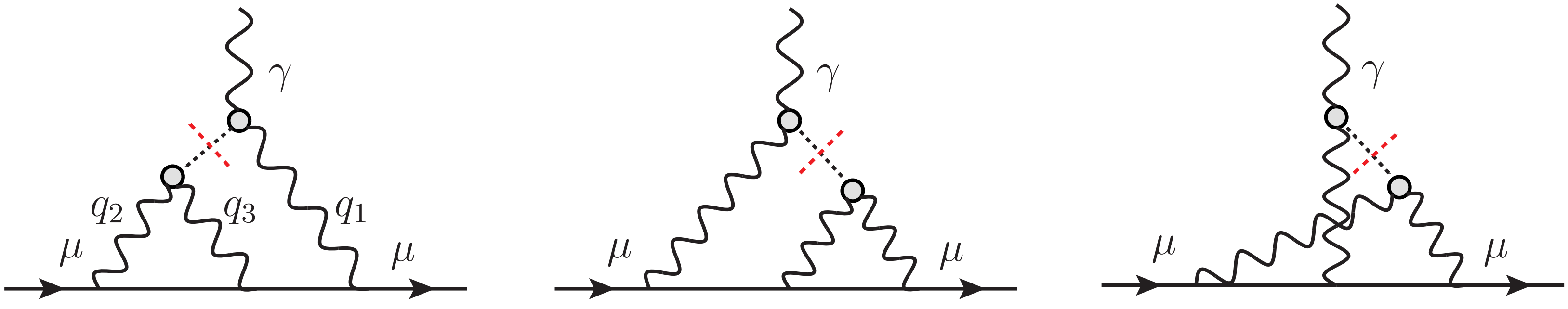

$$a_\mu^{\pi^0\text{-pole}} = \left(\frac{\alpha}{\pi}\right)^3 \int_0^\infty dQ_1 \int_0^\infty dQ_2 \int_{-1}^1 d\tau$$
$$\times \Big[w_1(Q_1,Q_2,\tau)\, F_{\pi^0\gamma^*\gamma^*}(-Q_1^2,-Q_3^2)\, F_{\pi^0\gamma^*\gamma^*}(-Q_2^2,0)$$
$$+ w_2(Q_1,Q_2,\tau)\, F_{\pi^0\gamma^*\gamma^*}(-Q_1^2,-Q_2^2)\, F_{\pi^0\gamma^*\gamma^*}(-Q_3^2,0) \Big]$$

- $w_{1/2}(Q_1,Q_2,\tau)$: kinematical weight functions, $\tau = \cos\theta$
- $F_{\pi^0\gamma^*\gamma^*}(-Q_1^2,-Q_2^2)$: space-like on-shell π^0 TFF

Pion-pole contribution to a_μ

- weight functions $w_{1/2}(Q_1, Q_2, \tau = 0)$: Nyffeler 2016

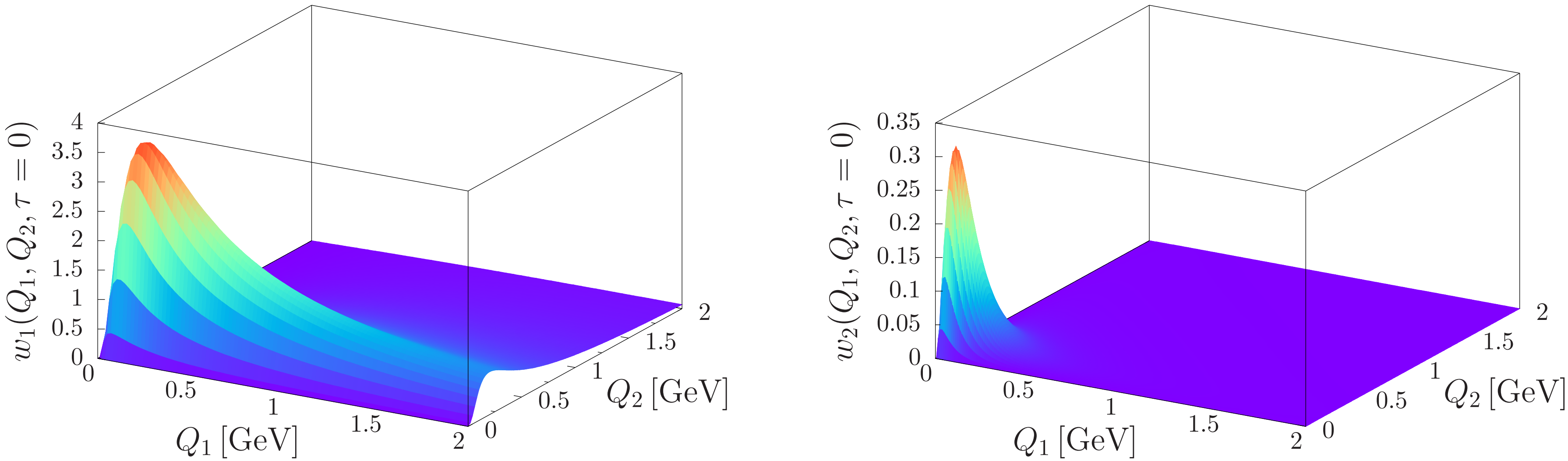

- concentrated for $Q_i \leq 0.5$ GeV
  $\longrightarrow$ pion-pole contribution dominantly from low-energy region
  $\longrightarrow$ pion transition form factor can be determined model-independently and with high precision using dispersion relations

Dispersive analysis of $\pi^0 \to \gamma^*\gamma^*$

- isospin decomposition:

$$F_{\pi^0\gamma^*\gamma^*}(q_1^2, q_2^2) = F_{vs}(q_1^2, q_2^2) + F_{vs}(q_2^2, q_1^2)$$

- analyse the leading hadronic intermediate states:

Hoferichter et al. 2014

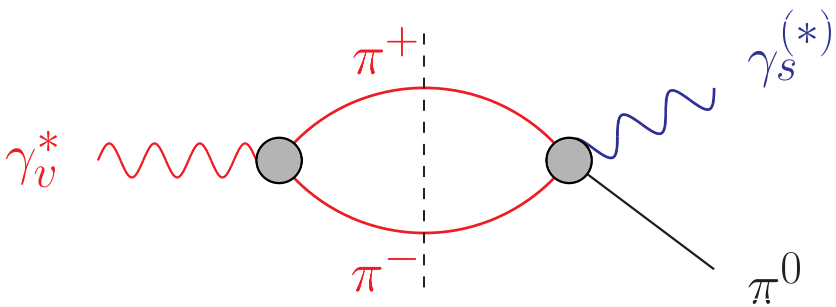

▷ isovector photon: 2 pions

$\propto$ pion vector form factor — very well known from $e^+e^- \to \pi^+\pi^-$

$\times$ $\gamma^* \to 3\pi$ P-wave amplitude — discussed next: Khuri–Treiman

Dispersive analysis of $\pi^0 \to \gamma^*\gamma^*$

- isospin decomposition:

$$F_{\pi^0\gamma^*\gamma^*}(q_1^2, q_2^2) = F_{vs}(q_1^2, q_2^2) + F_{vs}(q_2^2, q_1^2)$$

- analyse the leading hadronic intermediate states:

Hoferichter et al. 2014

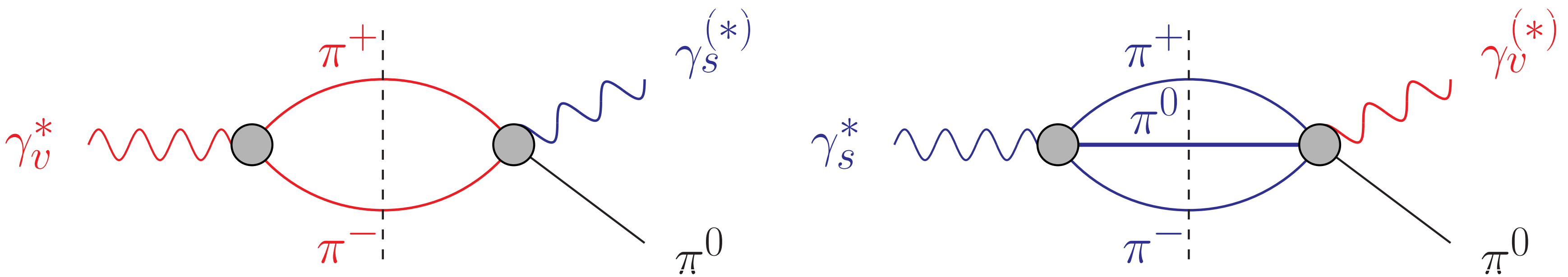

  ▷ isovector photon: 2 pions

    $\propto$ pion vector form factor — very well known from $e^+e^- \to \pi^+\pi^-$

    $\times$ $\gamma^* \to 3\pi$ P-wave amplitude — discussed next: Khuri–Treiman

  ▷ isoscalar photon: 3 pions

Dispersive analysis of $\pi^0 \to \gamma^*\gamma^*$

- isospin decomposition:

$$F_{\pi^0\gamma^*\gamma^*}(q_1^2, q_2^2) = F_{vs}(q_1^2, q_2^2) + F_{vs}(q_2^2, q_1^2)$$

- analyse the leading hadronic intermediate states:

Hoferichter et al. 2014

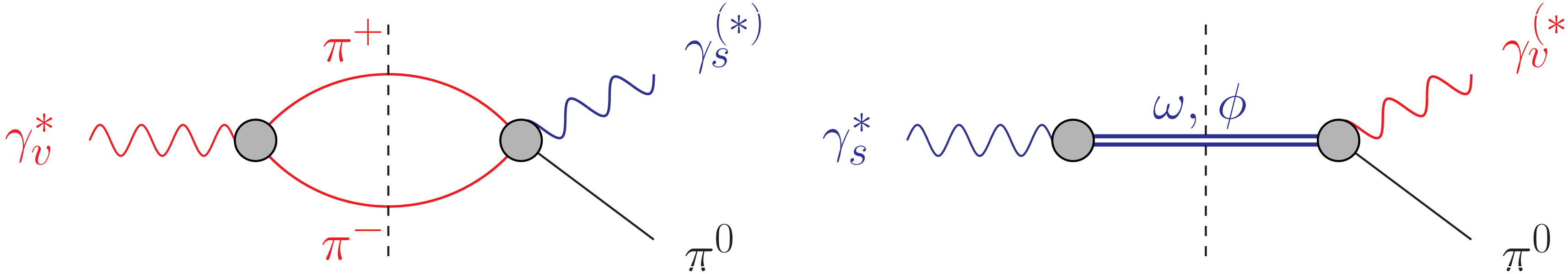

▷ isovector photon: 2 pions

$\propto$ pion vector form factor — very well known from $e^+e^- \to \pi^+\pi^-$

$\times$ $\gamma^* \to 3\pi$ P-wave amplitude — discussed next: Khuri–Treiman

▷ isoscalar photon: 3 pions

dominated by narrow resonances ω, ϕ

Khuri–Treiman representation $\gamma^* \to 3\pi$

cf. talk by E. Passemar on $\eta \to 3\pi$

- $\gamma^*(q^2) \to 3\pi$: crossing symmetric $s \leftrightarrow t \leftrightarrow u$ P-wave isobars

$$\mathcal{F}(s,t,u;q^2) = \mathcal{F}(s,q^2) + \mathcal{F}(t,q^2) + \mathcal{F}(u,q^2)$$

- WZW low-energy theorem $\mathcal{F}(0,0,0;0) = F_{3\pi} = \dfrac{1}{4\pi^2 F_\pi^3}$

Khuri–Treiman representation $\gamma^* \to 3\pi$

cf. talk by E. Passemar on $\eta \to 3\pi$

- $\gamma^*(q^2) \to 3\pi$: crossing symmetric $s \leftrightarrow t \leftrightarrow u$ P-wave isobars

$$\mathcal{F}(s,t,u;q^2) = \mathcal{F}(s,q^2) + \mathcal{F}(t,q^2) + \mathcal{F}(u,q^2)$$

- WZW low-energy theorem $\quad \mathcal{F}(0,0,0;0) = F_{3\pi} = \dfrac{1}{4\pi^2 F_\pi^3}$

- (s-channel) P-wave projection: $f_1(s,q^2) = \mathcal{F}(s,q^2) + \hat{\mathcal{F}}(s,q^2)$

  $\hat{\mathcal{F}}(s,q^2)$: contribution from crossed channels

- left-hand cut $\hat{\mathcal{F}}(s,q^2)$ and right-hand cut $\mathcal{F}(s,q^2)$ self-consistent:

$$\mathcal{F}(s,q^2) = \underbrace{\Omega(s)}_{\text{Omnès}} \left\{ a(q^2) + \frac{s}{\pi} \int_{4M_\pi^2}^{\infty} \frac{ds'}{s'} \frac{\sin \delta_1^1(s') \hat{\mathcal{F}}(s',q^2)}{|\Omega(s')|(s'-s)} \right\}$$

$=$ 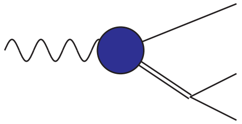 $+$ 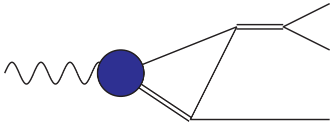 $+$ 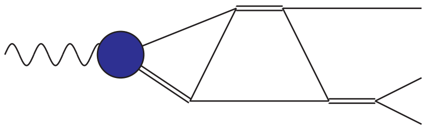 $+ \ \ldots$

$\longrightarrow$ pairwise rescattering to all orders

Hoferichter et al. 2014

From $e^+e^- \to 3\pi$ to $e^+e^- \to \pi^0\gamma^*$

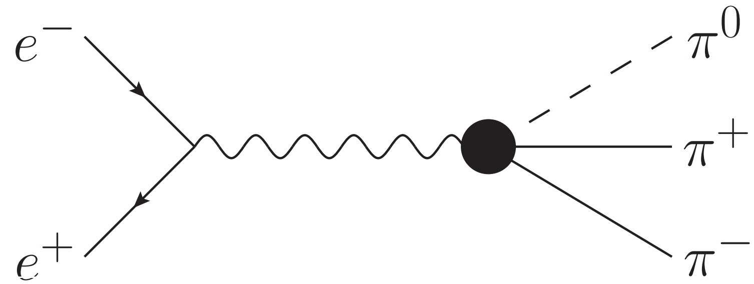

- amplitude for $e^+e^- \to 3\pi \quad \propto \mathcal{F}(s,q^2) + \mathcal{F}(t,q^2) + \mathcal{F}(u,q^2)$

$$\mathcal{F}(s,q^2) = \Omega(s)\left\{a(q^2) + \frac{s}{\pi}\int_{4M_\pi^2}^{\infty}\frac{ds'}{s'}\frac{\sin\delta_1^1(s')\hat{\mathcal{F}}(s',q^2)}{|\Omega(s')|(s'-s)}\right\}$$

subtraction function $a(q^2)$ adjusted to reproduce $e^+e^- \to 3\pi$

- parameterisation:

$$a(q^2) = \frac{F_{3\pi}}{3} + \frac{q^2}{\pi}\int_{\mathrm{thr}}^{\infty} ds' \frac{\mathrm{Im}BW(s')}{s'(s'-q^2)} + C_n(q^2)$$

$BW(q^2)$: poles ω, ϕ, ω'; $C_n(q^2)$: conformal pol. $\longrightarrow$ inelasticities

From $e^+e^- \to 3\pi$ to $e^+e^- \to \pi^0\gamma^*$

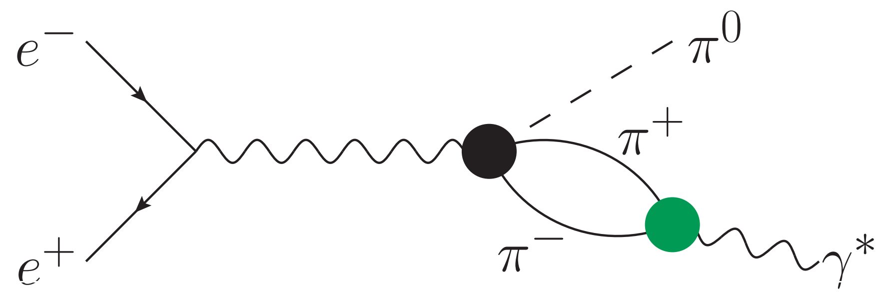

- amplitude for $e^+e^- \to 3\pi \quad \propto \mathcal{F}(s,q^2) + \mathcal{F}(t,q^2) + \mathcal{F}(u,q^2)$

$$\mathcal{F}(s,q^2) = \Omega(s)\left\{a(q^2) + \frac{s}{\pi}\int_{4M_\pi^2}^{\infty}\frac{ds'}{s'}\frac{\sin\delta_1^1(s')\hat{\mathcal{F}}(s',q^2)}{|\Omega(s')|(s'-s)}\right\}$$

subtraction function $a(q^2)$ adjusted to reproduce $e^+e^- \to 3\pi$

- parameterisation:

$$a(q^2) = \frac{F_{3\pi}}{3} + \frac{q^2}{\pi}\int_{\mathrm{thr}}^{\infty} ds' \frac{\mathrm{Im}BW(s')}{s'(s'-q^2)} + C_n(q^2)$$

$BW(q^2)$: poles ω, ϕ, ω'; $C_n(q^2)$: conformal pol. $\longrightarrow$ inelasticities

- fit to $e^+e^- \to 3\pi$ data $\longrightarrow$ prediction for $e^+e^- \to \pi^0\gamma^{(*)}$

Fit results $e^+e^- \to 3\pi$ data up to 1.8 GeV

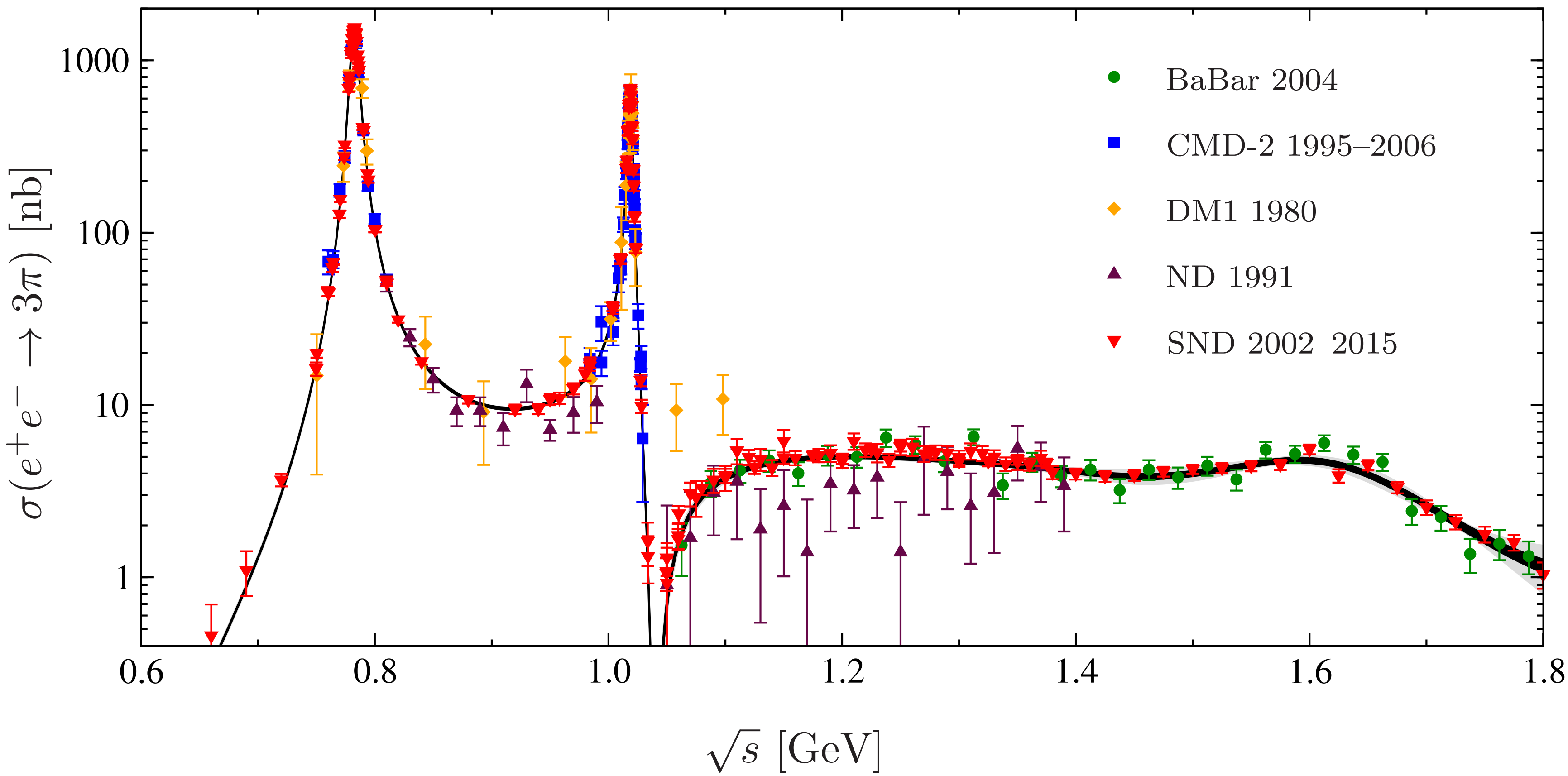

Hoferichter, Hoid, BK 2019

- black / gray bands represent fit and total uncertainties
- vacuum polarisation removed from the cross section

Fit results: 3π contribution to HVP

- second largest exclusive channel next to $\pi^+\pi^-$
- central result for the 3π contribution to HVP:

$$\boxed{a_\mu^{3\pi}|_{\leq 1.8\,\text{GeV}} = 462(6)(6) \times 10^{-11} = 462(8) \times 10^{-11}}$$

Hoferichter, Hoid, BK 2019

- independent cross-check with dispersion-theoretical amplitude:

analyticity, unitarity, QCD constraints

Davier et al. 2017, 2019	Keshavarzi et al. 2018	Jegerlehner 2017
$462.0(14.5)$	$477.0(8.9)$	$443(15)$

- analogous to $\pi^+\pi^-$ Colangelo, Hoferichter, Stoffer 2018

Comparison to $e^+e^- \to \pi^0\gamma$ data; HVP

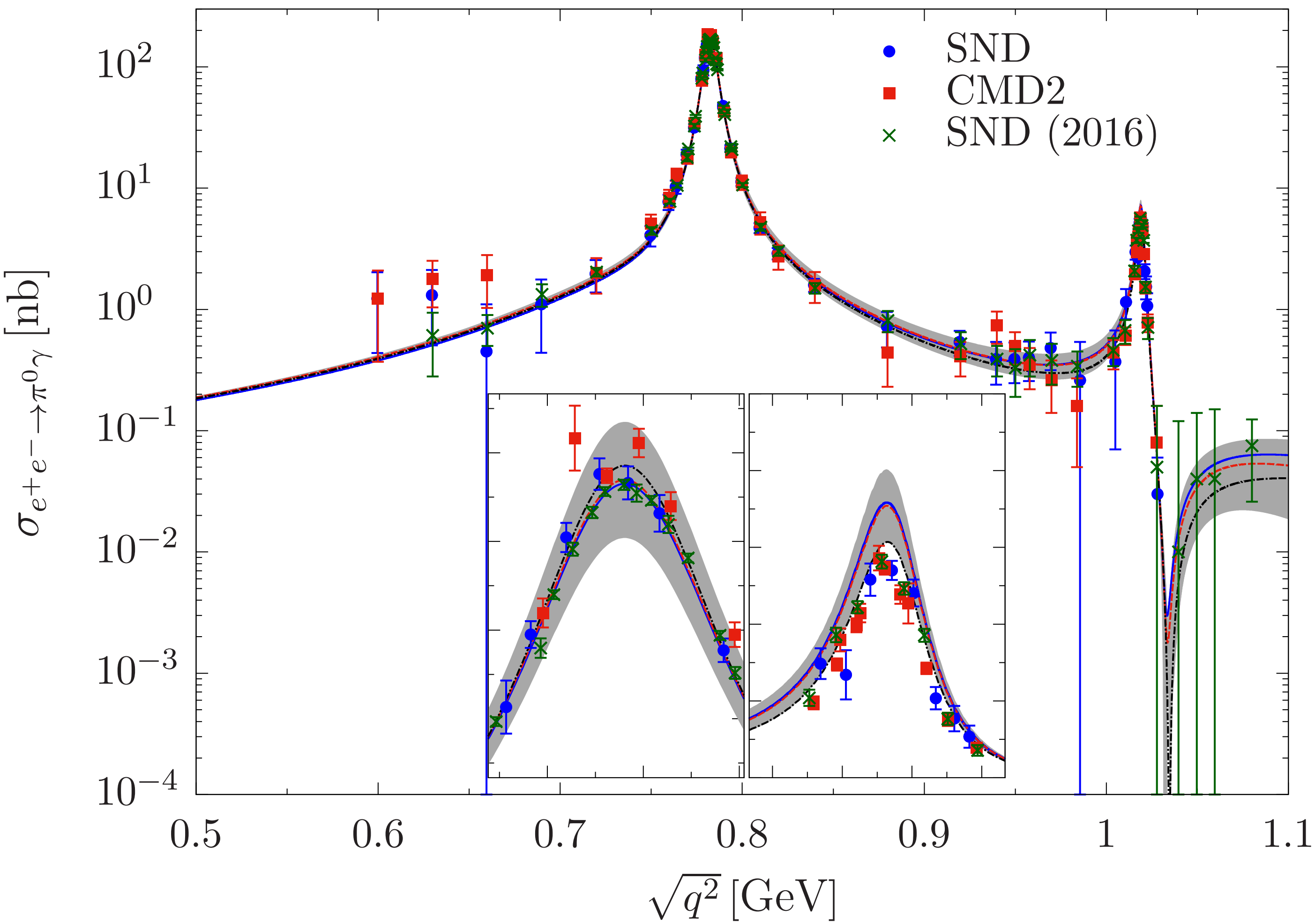

Hoferichter, Hoid, BK, Leupold, Schneider 2018

- “prediction”—no further parameters adjusted
- data very well reproduced

Comparison to $e^+e^- \to \pi^0\gamma$ data; HVP

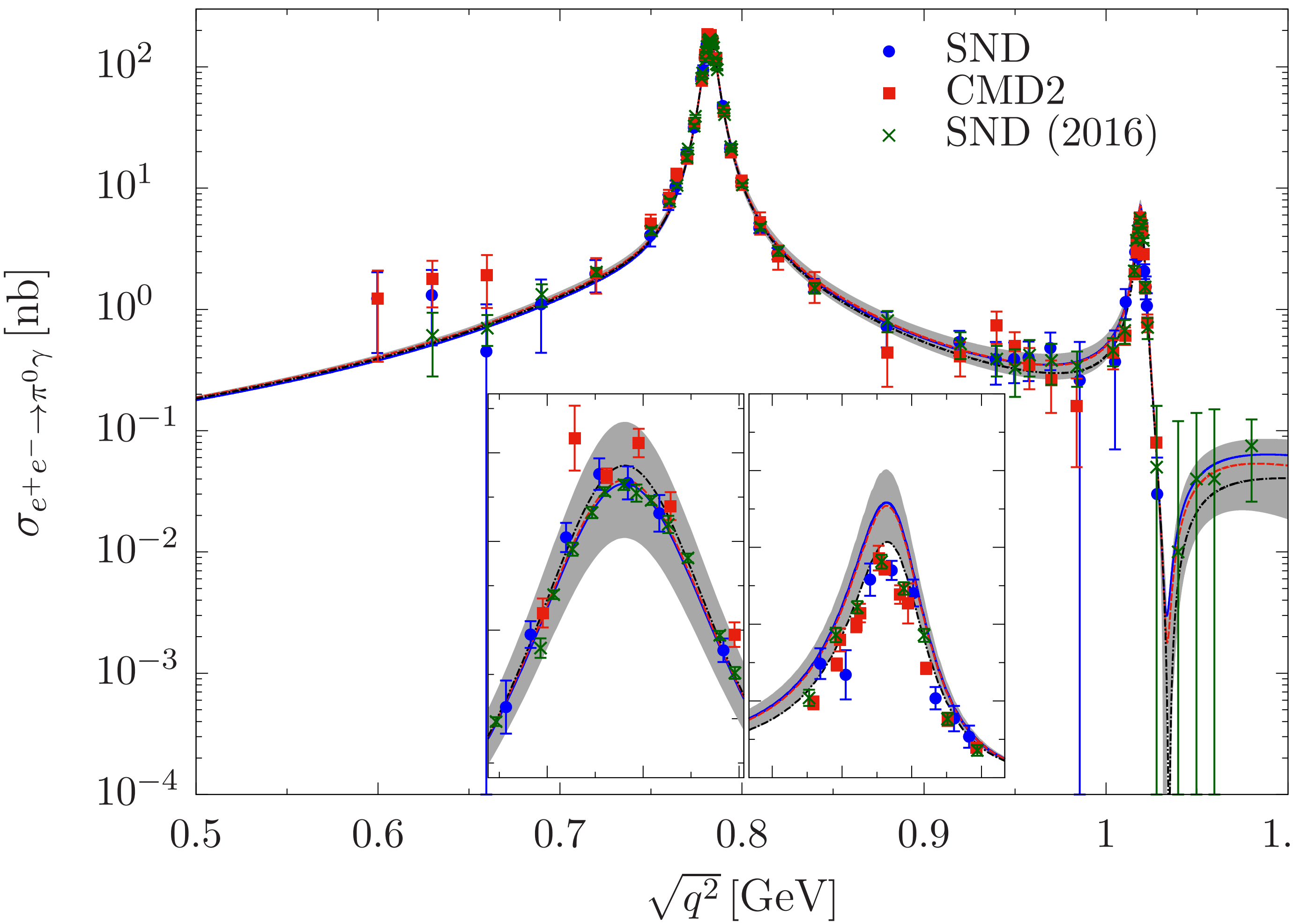

- fit instead for $\pi^0\gamma$ HVP contribution: Hoid, Hoferichter, BK 2020

$$\boxed{a_\mu^{\pi^0\gamma}|_{\leq 1.35\,\mathrm{GeV}} = 43.8(6)(1) \times 10^{-11} = 43.8(6) \times 10^{-11}}$$

Asymptotics and pQCD constraints (1)

- so far: dispersion relation based on (dominant) 2π, 3π
  $\longrightarrow$ high precision at low energies
- double-spectral-function representation:

$$F_{\pi^0\gamma^*\gamma^*}(q_1^2,q_2^2) = \frac{1}{\pi^2}\int_{4M_\pi^2}^\infty dx \int_{s_{\rm thr}}^\infty dy \frac{\rho^{\rm disp}(x,y)}{(x-q_1^2)(y-q_2^2)}$$

$$\rho^{\rm disp}(x,y) = \frac{q_\pi^3(x)}{12\pi\sqrt{x}}{\rm Im}\left[F_\pi^{V*}(x)f_1(x,y)\right] + [x \leftrightarrow y]$$

Asymptotics and pQCD constraints (1)

- so far: dispersion relation based on (dominant) 2π, 3π
  $\longrightarrow$ high precision at low energies
- double-spectral-function representation:

$$F_{\pi^0\gamma^*\gamma^*}(q_1^2,q_2^2) = \frac{1}{\pi^2}\int_{4M_\pi^2}^{\infty} dx \int_{s_{\text{thr}}}^{\infty} dy \frac{\rho^{\text{disp}}(x,y)}{(x-q_1^2)(y-q_2^2)}$$

$$\rho^{\text{disp}}(x,y) = \frac{q_\pi^3(x)}{12\pi\sqrt{x}} \text{Im}\left[F_\pi^{V*}(x) f_1(x,y)\right] + [x \leftrightarrow y]$$

- asymptotically: pion wave function $\phi_\pi(x) = 6x(1-x) + \ldots$

$$F_{\pi^0\gamma^*\gamma^*}(q_1^2,q_2^2) = -\frac{2F_\pi}{3}\int_0^1 dx \frac{\phi_\pi(x)}{xq_1^2+(1-x)q_2^2} + \mathcal{O}\big(Q^{-4}\big)$$

  implies asymptotically — Brodsky, Lepage 1979–1981

$$F_{\pi^0\gamma^*\gamma^*}\big(-Q^2,-Q^2\big) \sim \frac{2F_\pi}{3Q^2}\,, \qquad F_{\pi^0\gamma^*\gamma^*}\big(-Q^2,0\big) \sim \frac{2F_\pi}{Q^2}$$

  $\longrightarrow$ rewrite this as double-spectral representation $\rho^{\text{pQCD}}(x,y)$
  Khodjamirian 1999; Hoferichter et al. 2018

Asymptotics and pQCD constraints (2)

- dispersion-theoretical $\rho^{\text{disp}}(x,y)$ at low energies $x,y \leq s_m$
- doubly-asymptotic $\rho^{\text{pQCD}}(x,y)$ for $x,y > s_m$
  $\longrightarrow$ does not contribute to singly-virtual TFF

$$F_{\pi^0\gamma^*\gamma^*}(q_1^2,q_2^2) = \frac{1}{\pi^2}\int_0^{s_\text{m}} dx \int_0^{s_\text{m}} dy \frac{\rho^{\text{disp}}(x,y)}{(x-q_1^2)(y-q_2^2)} + \frac{1}{\pi^2}\int_{s_\text{m}}^{\infty} dx \int_{s_\text{m}}^{\infty} dy \frac{\rho^{\text{pQCD}}(x,y)}{(x-q_1^2)(y-q_2^2)}$$

- pQCD piece alone: $\quad F_{\pi^0\gamma^*\gamma^*}\big(-Q^2,-Q^2\big) = \frac{2F_\pi}{3Q^2} + \mathcal{O}\big(Q^{-4}\big)$

  dispersive part: $\quad \frac{1}{\pi^2}\int_0^{s_\text{m}} dx \int_0^{s_\text{m}} dy \frac{\rho^{\text{disp}}(x,y)}{(x+Q^2)(y+Q^2)} = \mathcal{O}\big(Q^{-4}\big)$

Asymptotics and pQCD constraints (2)

- dispersion-theoretical $\rho^{\text{disp}}(x,y)$ at low energies $x,y \leq s_m$
- doubly-asymptotic $\rho^{\text{pQCD}}(x,y)$ for $x,y > s_m$
  $\longrightarrow$ does not contribute to singly-virtual TFF

$$F_{\pi^0\gamma^*\gamma^*}(q_1^2,q_2^2) = \frac{1}{\pi^2}\int_0^{s_\text{m}} dx \int_0^{s_\text{m}} dy \frac{\rho^{\text{disp}}(x,y)}{(x-q_1^2)(y-q_2^2)} + \frac{1}{\pi^2}\int_{s_\text{m}}^{\infty} dx \int_{s_\text{m}}^{\infty} dy \frac{\rho^{\text{pQCD}}(x,y)}{(x-q_1^2)(y-q_2^2)}$$

- pQCD piece alone: $F_{\pi^0\gamma^*\gamma^*}\big(-Q^2,-Q^2\big) = \dfrac{2F_\pi}{3Q^2} + \mathcal{O}\big(Q^{-4}\big)$

  dispersive part: $\displaystyle\frac{1}{\pi^2}\int_0^{s_\text{m}} dx \int_0^{s_\text{m}} dy \frac{\rho^{\text{disp}}(x,y)}{(x+Q^2)(y+Q^2)} = \mathcal{O}\big(Q^{-4}\big)$

- anomaly and Brodsky–Lepage: $\rho^{\text{disp}}(x,y)$ fulfils two sum rules

  $\longrightarrow$ add effective pole: $\rho^{\text{eff}} = \dfrac{g_\text{eff}}{4\pi^2 F_\pi}\pi^2 M_\text{eff}^4 \delta\big(x-M_\text{eff}^2\big)\delta\big(y-M_\text{eff}^2\big)$

  find $g_\text{eff} \sim 10\%$ (small), $M_\text{eff} \sim 1.5\ldots2.0\,\text{GeV}$ (reasonable)

Uncertainties in the π^0 pole contribution

Normalisation

- uncertainty on $\pi^0 \to \gamma\gamma$ $\pm 1.5\%$ PrimEx 2020

Dispersive input

- different $\pi\pi$ phase shift inputs:
  - ▷ Bern vs. Madrid Colangelo et al. 2011, García-Martín et al. 2011
  - ▷ effective form factor phase (incl. ρ', ρ'') Schneider et al. 2012
- cutoff in Khuri–Treiman integrals $1.8 \ldots 2.5\,\mathrm{GeV}$

Brodsky–Lepage limit uncertainty

- allow for ${}^{+20\%}_{-10\%}$, 3σ band around data BaBar 2009, Belle 2012

Onset of pQCD asymptotics

- vary $s_m = 1.7(3)$GeV^2

Results: singly-virtual

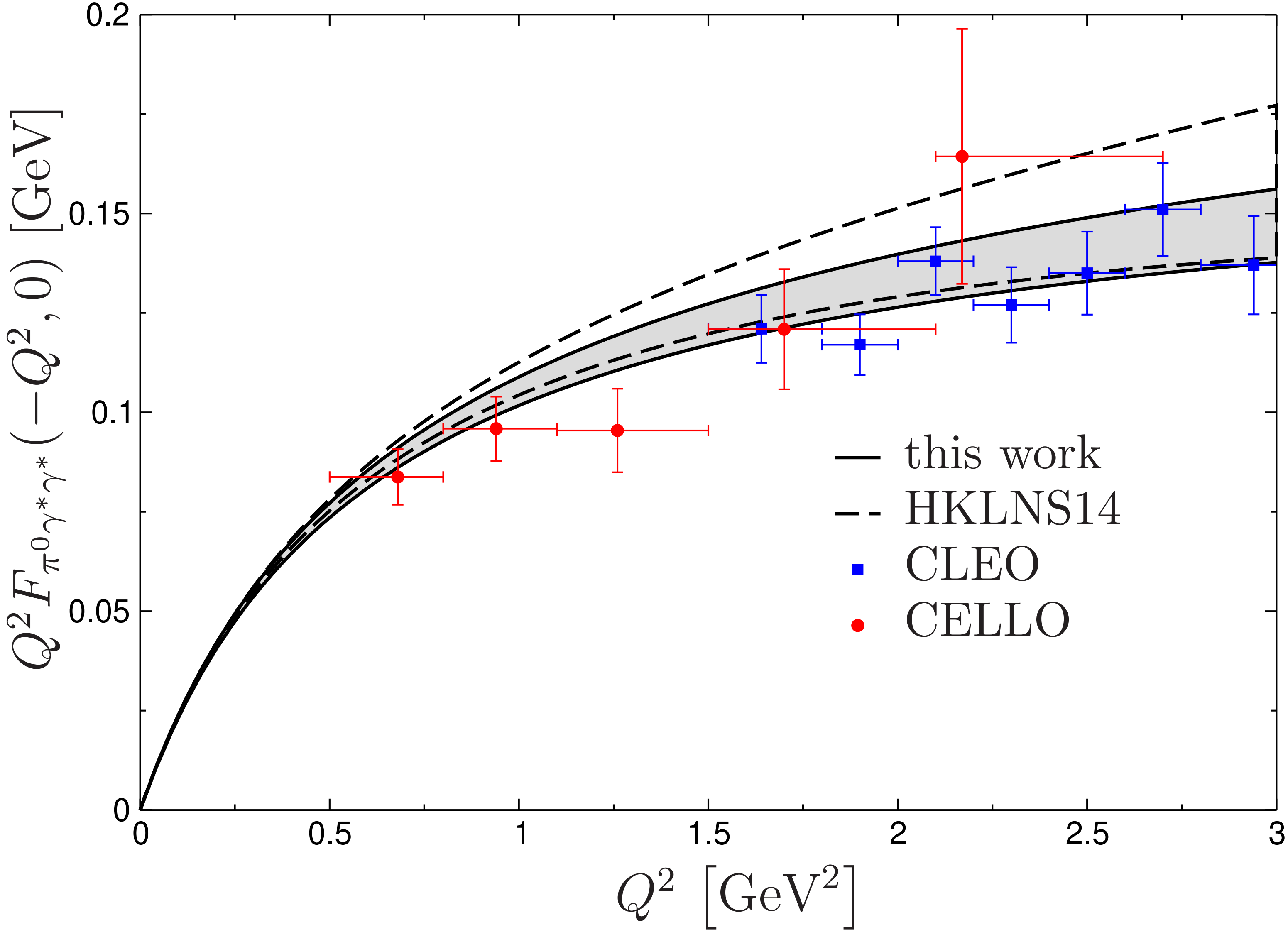

Hoferichter, Hoid, BK, Leupold, Schneider 2018

Results: singly-virtual

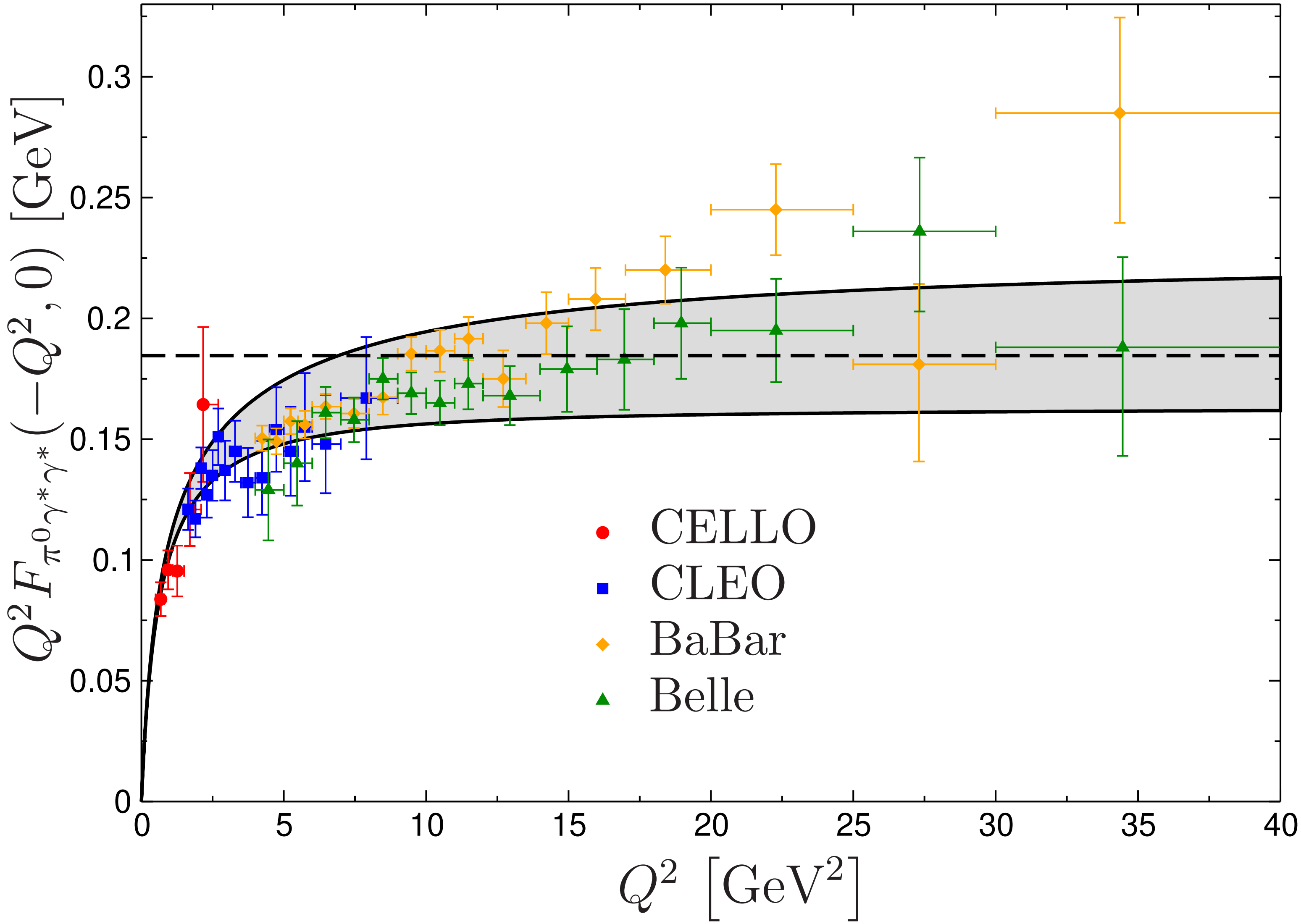

Hoferichter, Hoid, BK, Leupold, Schneider 2018

Comparison dispersive vs. LMD+V-lattice

- plot $\left(Q_1^2+Q_2^2\right)F_{\pi^0\gamma^*\gamma^*}\left(-Q_1^2,-Q_2^2\right)$:

dispersive

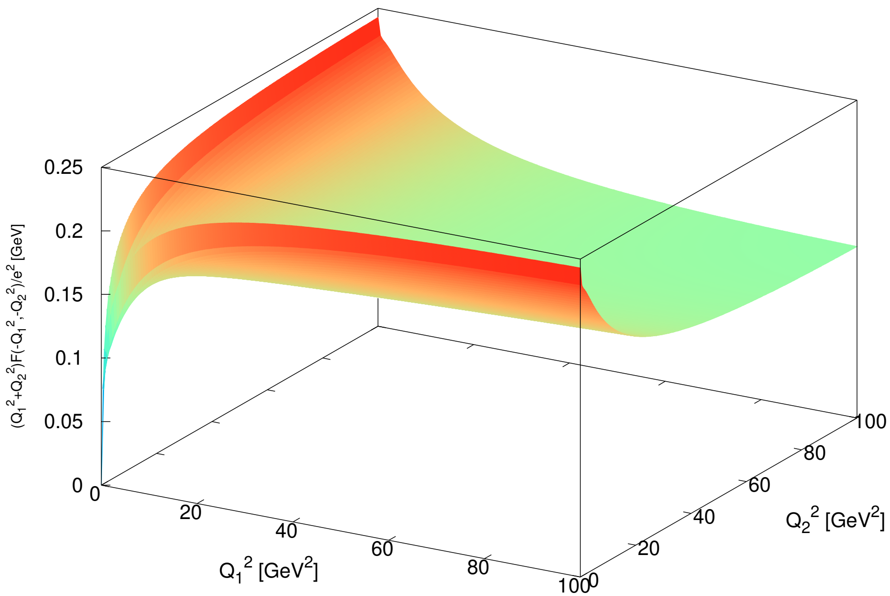

Hoferichter, Hoid, BK, Leupold, Schneider 2018

LMD+V fit to lattice

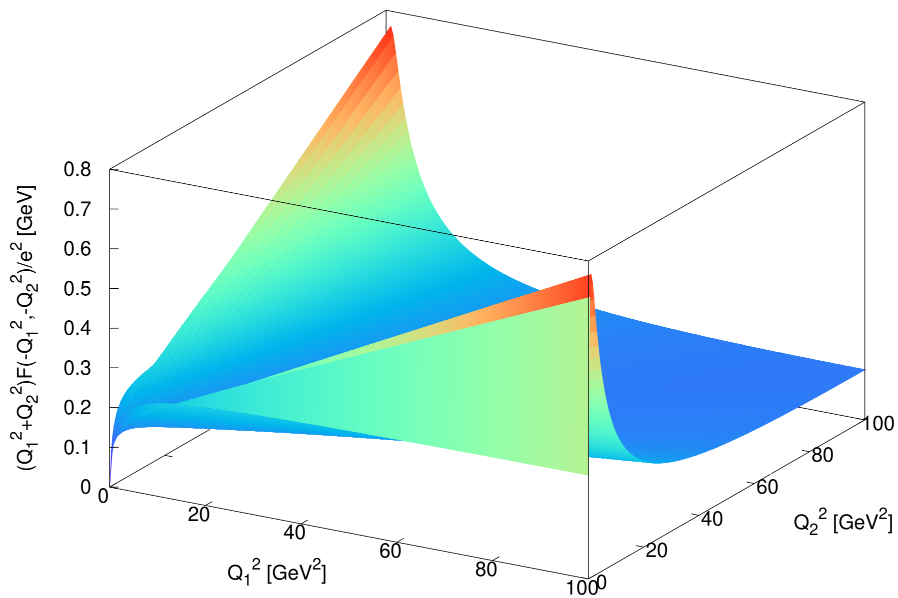

Gérardin, Meyer, Nyffeler 2016

Result: $(g-2)_\mu$ from π^0 pole

Final result for the π^0 pole contribution $[10^{-11}]$

63.0 ± 0.9	chiral anomaly / $\pi^0 \to \gamma\gamma$
± 1.1	dispersive input
${}^{+2.2}_{-1.4}$	Brodsky–Lepage
± 0.6	onset of pQCD contribution s_m
$= 63.0\,{}^{+2.7}_{-2.1}$	Hoferichter, Hoid, BK, Leupold, Schneider 2018

- model-independent, data-driven determination
  with all physical low- and high-energy constraints implemented
- perfectly consistent with
  - ▷ Padé approxim. $63.6(2.7) \times 10^{-11}$ Masjuan, Sánchez-Puertas 2017
  - ▷ lattice $62.3(2.3) \times 10^{-11}$ Gérardin et al. 2019

“White Paper” summary HLbL

hadronic state	$a_\mu^{\mathrm{HLbL}}\ [10^{-11}]$	
pseudoscalar poles	$93.8^{+4.0}_{-3.6}$	η, η': Masjuan, Sánchez-Puertas 2017
pion box	$-15.9(2)$	Colangelo et al. 2017
S-wave $\pi\pi$ rescatt.	$-8(1)$	Colangelo et al. 2017
kaon box	$-0.5(1)$	
scalars+tensors $\gtrsim 1\,\mathrm{GeV}$	$\sim -1(3)$	
axial vectors	$\sim 6(6)$	
short distance	$\sim 15(10)$	
heavy quarks	$\sim 3(1)$	
total	$92(19)$	Aoyama et al. 2020

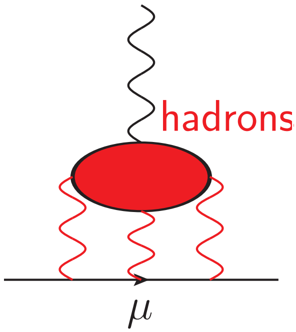

$\longrightarrow$ further need for improvement to reach 10% accuracy for a_μ^{HLbL}

$\longrightarrow$ see talk by P. Sánchez-Puertas

Summary / Outlook

Dispersive analysis of π^0 transition form factor:

- based on high-precision data on $e^+e^- \to \pi^+\pi^-,\ \pi^+\pi^-\pi^0$
- matched onto all fundamental constraints:

  anomaly   Brodsky–Lepage limit   pQCD limit

- π^0 pole $(g-2)_\mu^{\pi^0} = 63.0^{+2.7}_{-2.1} \times 10^{-11}$

  uncertainties: $\pi^0 \to \gamma\gamma$ PrimEx-II

  dispersive uncertainties BES III

  BL limit (BaBar vs. Belle) Belle II

- further spinoff: $\pi^0 \to e^+e^-$ Hoferichter, Hoid, BK, Lüdtke 2021

In progress:

- similar program for η / η' Holz et al.; cf. also Gan, BK, Passemar, Tulin 2020

Main challenges for HLbL at 10% accuracy:

- axial vectors & short-distance constraints various

Spares

Results π^0 TFF: doubly-virtual (diagonal)

in comparison to Gérardin, Meyer, Nyffeler 2016

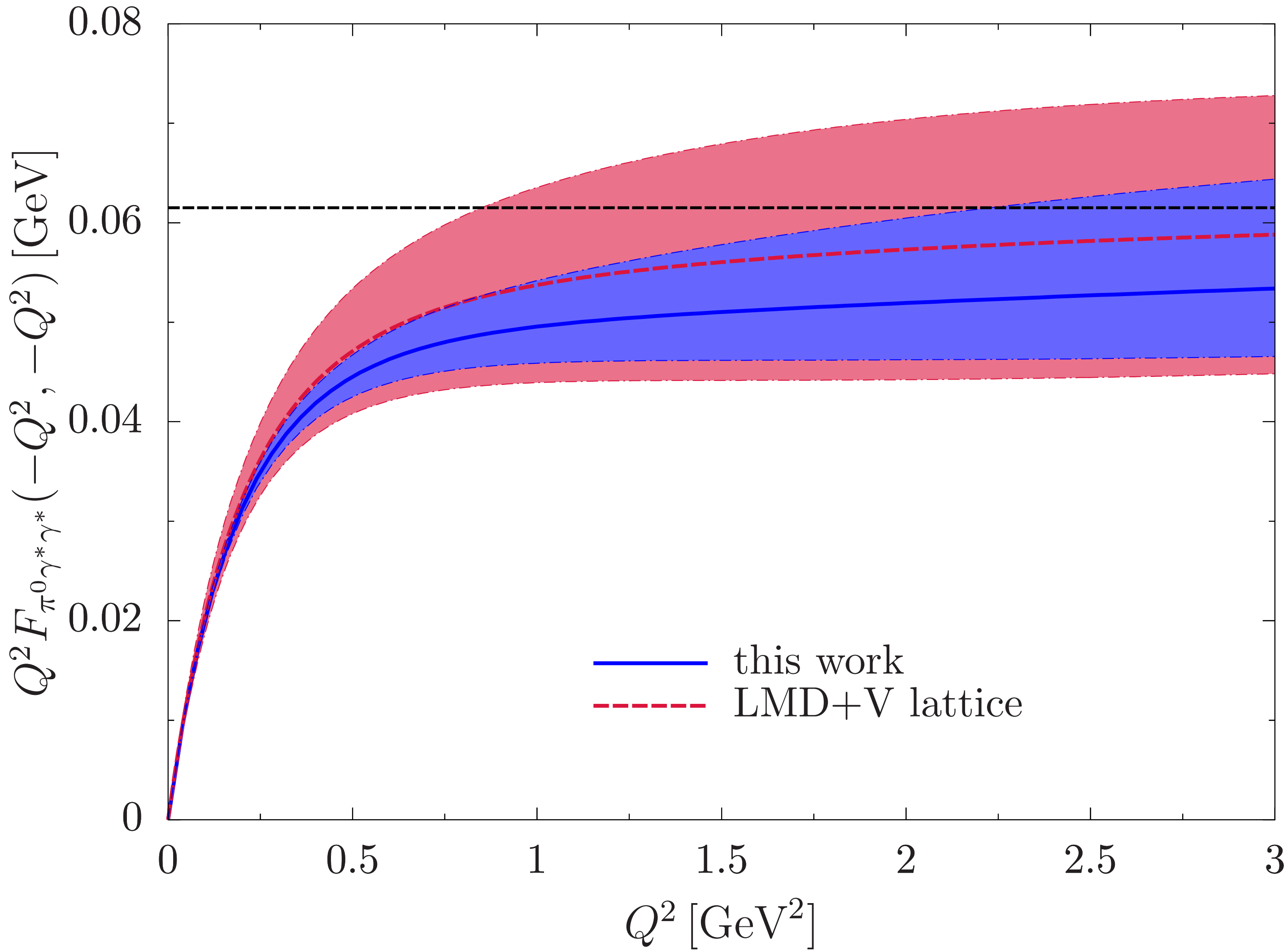

Hoferichter, Hoid, BK, Leupold, Schneider 2018

Results π^0 TFF: doubly-virtual (diagonal)

in comparison to Gérardin, Meyer, Nyffeler 2016

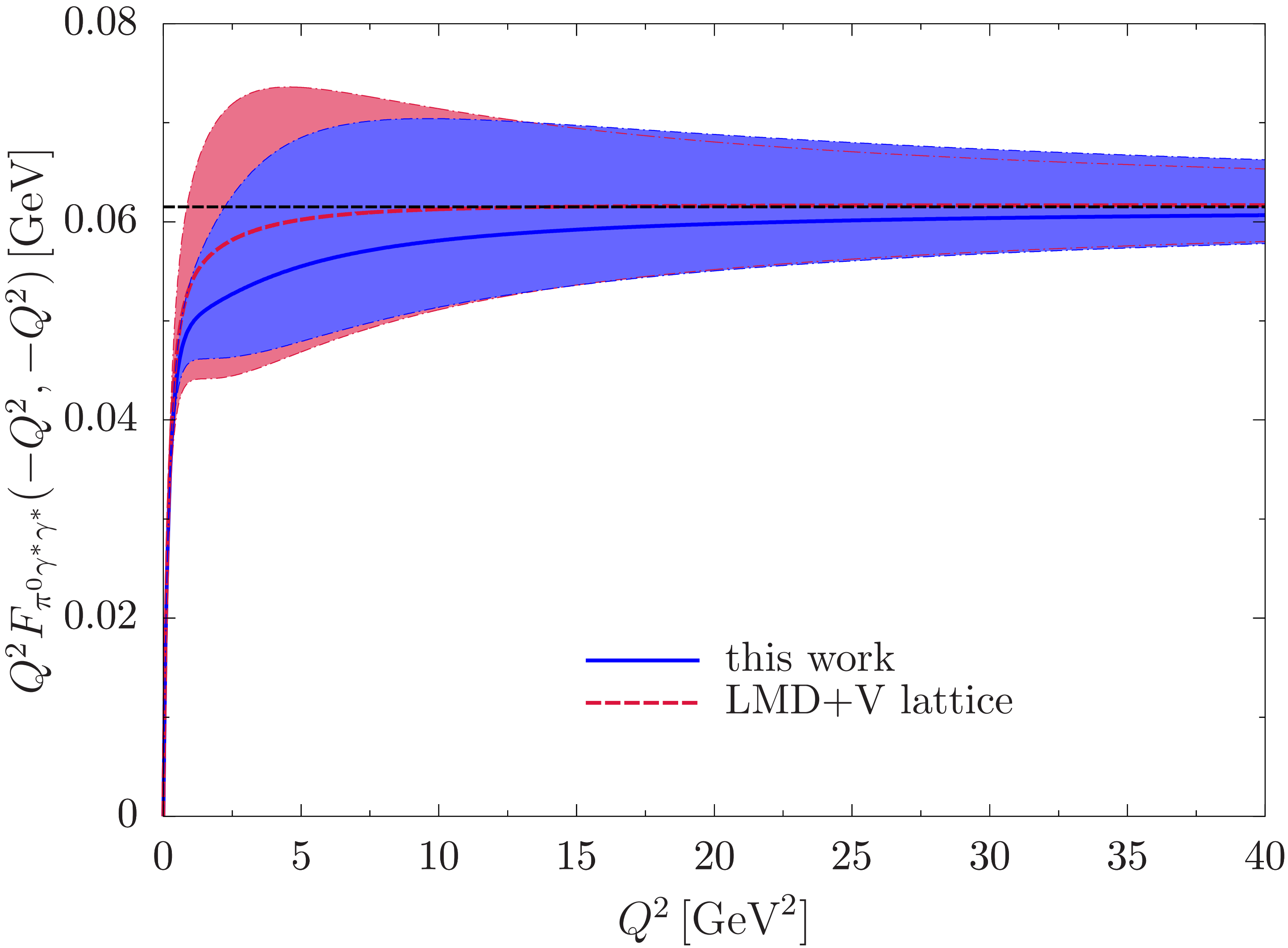

Hoferichter, Hoid, BK, Leupold, Schneider 2018

$\pi^0 \to \gamma^*\gamma^*$ transition form factor

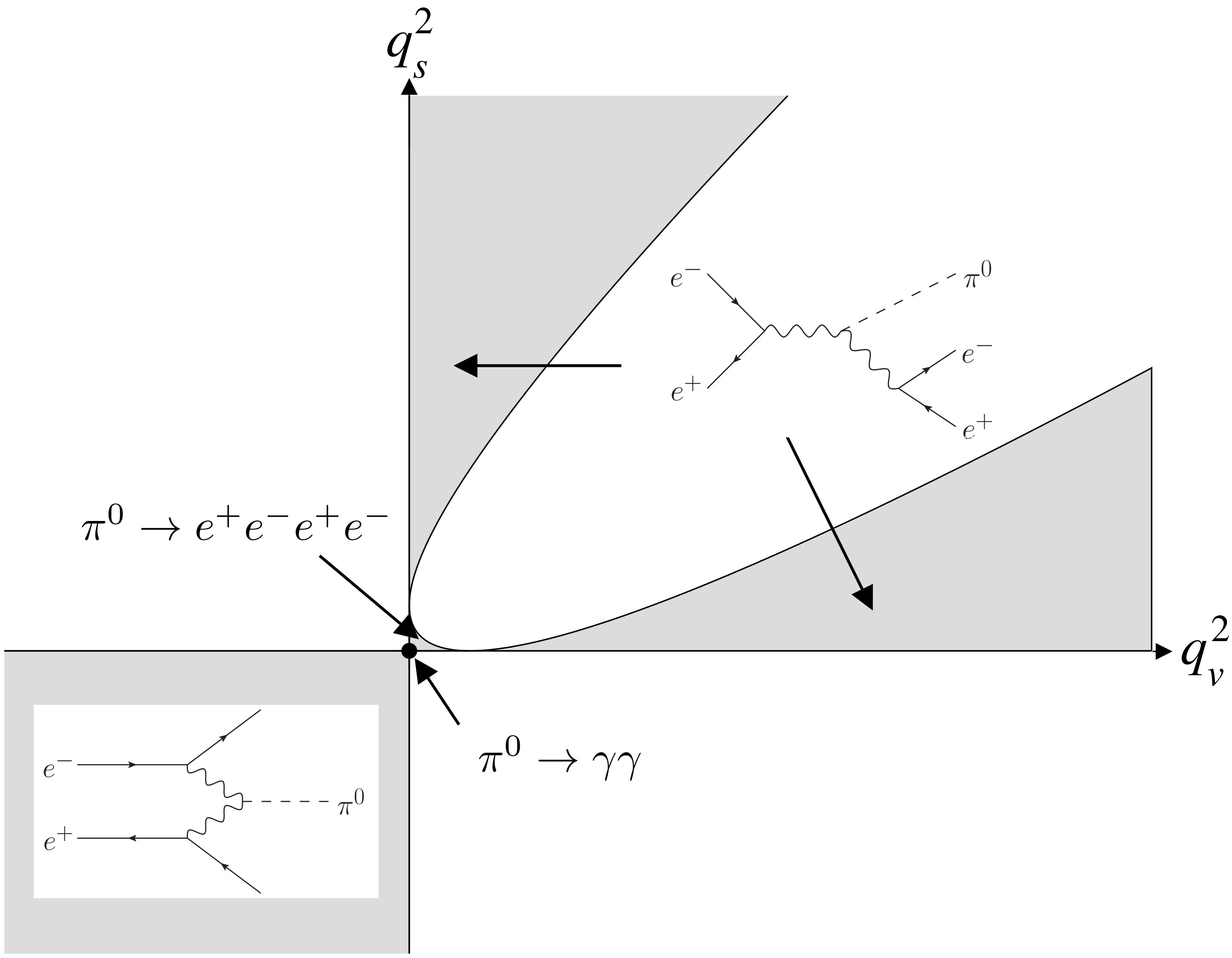

$\pi^0 \to \gamma^*\gamma^*$ transition form factor

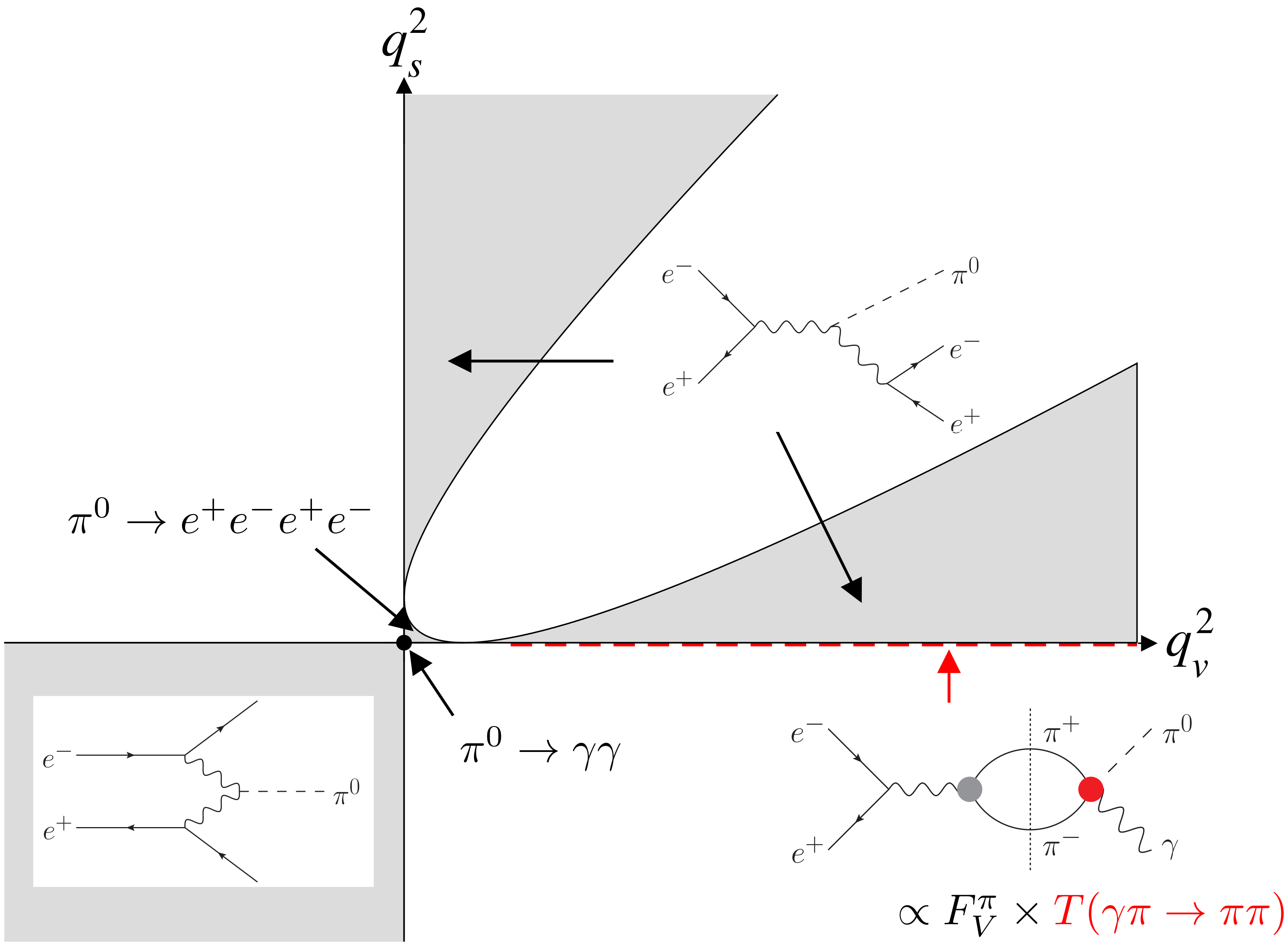

$\pi^0 \to \gamma^*\gamma^*$ transition form factor

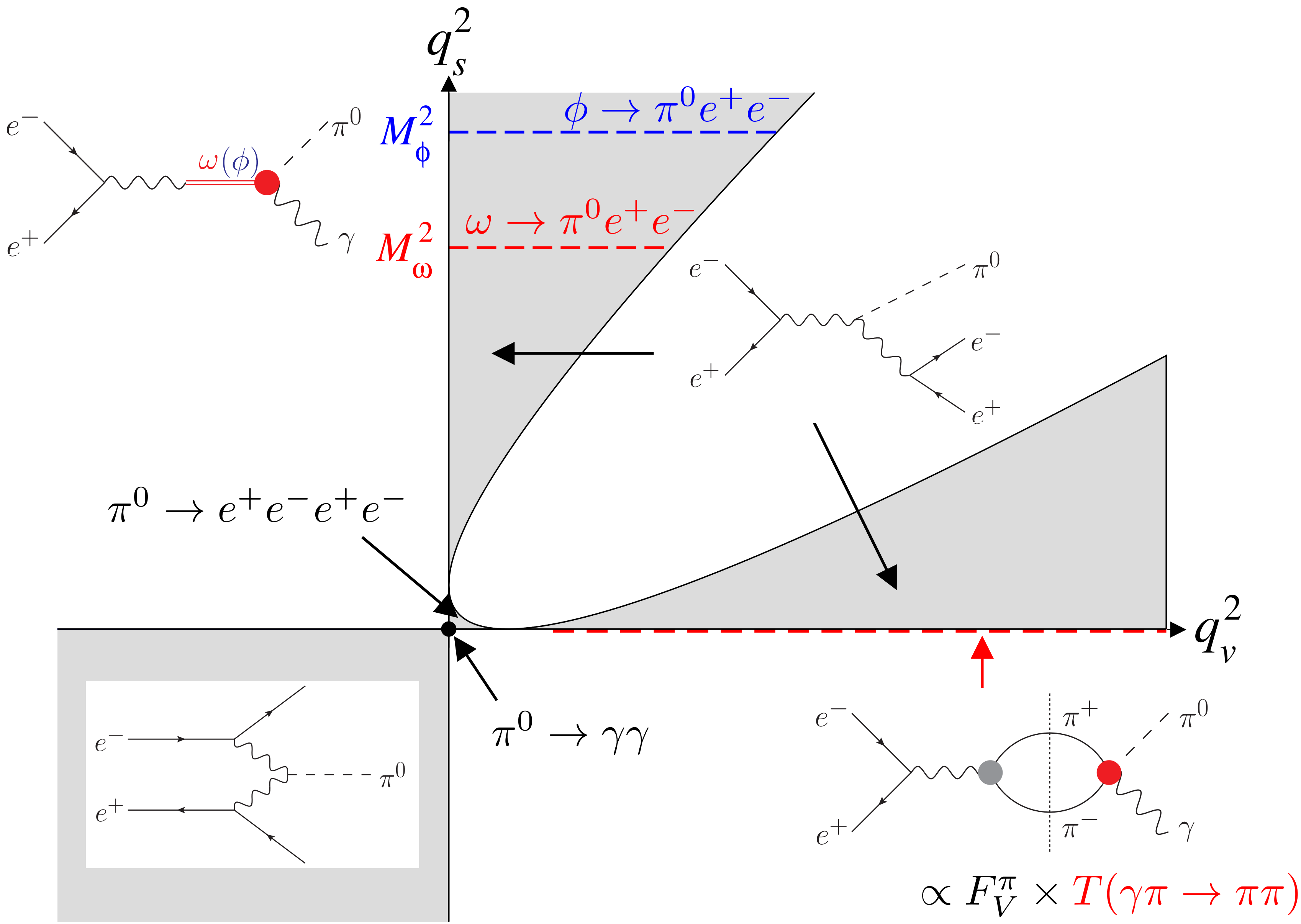

Pion vector form factor vs. Omnès representation

Data on pion form factor in $\tau^- \to \pi^- \pi^0 \nu_\tau$ Belle 2008

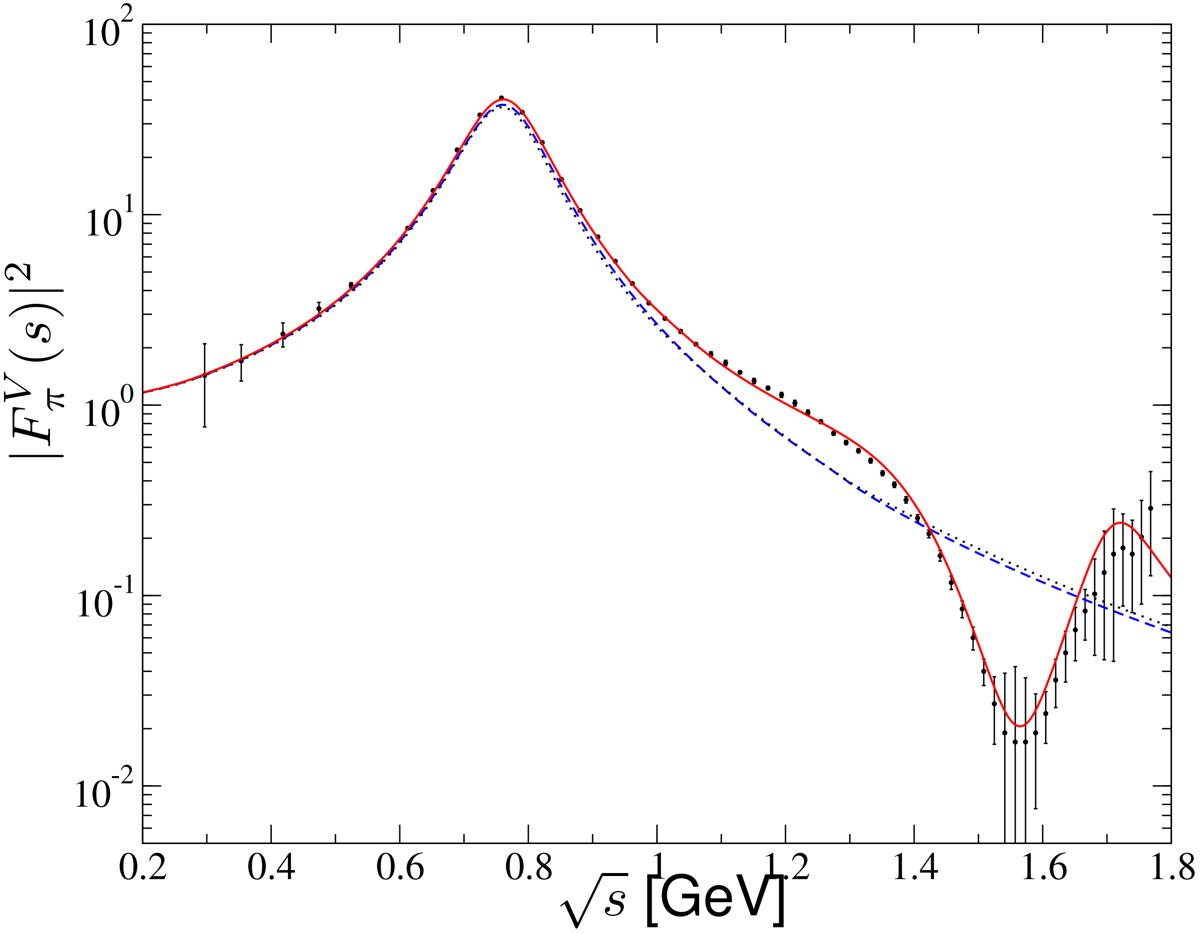

$\pi\pi$ P-wave phase shift / effective form factor phase incl. ρ', ρ''

Schneider et al. 2012

Dispersive representation $\gamma^* \to 3\pi$

- parameterisation of subtraction function $a(q^2)$

  $\longrightarrow$ to be fitted to $e^+e^- \to 3\pi$ cross section data:

$$a(q^2) = \frac{F_{3\pi}}{3} + \frac{q^2}{\pi}\int_{\rm thr}^{\infty} ds' \frac{\operatorname{Im}\mathcal{A}(s')}{s'(s'-q^2)} + C_n(q^2)$$

- $\mathcal{A}(q^2)$ includes resonance poles:

$$\mathcal{A}(q^2) = \sum_V \frac{c_V}{M_V^2 - q^2 - i\sqrt{q^2}\Gamma_V(q^2)} \qquad V = \omega, \phi, \omega', \omega''$$

  c_V real

- conformal polynomial (inelasticities); S-wave cusp eliminated:

$$C_n(q^2) = \sum_{i=1}^{n} c_i\Big(z(q^2)^i - z(0)^i\Big), \qquad z(q^2) = \frac{\sqrt{s_{\text{inel}} - s_1} - \sqrt{s_{\text{inel}} - q^2}}{\sqrt{s_{\text{inel}} - s_1} + \sqrt{s_{\text{inel}} - q^2}}$$

- exact implementation of $\gamma^* \to 3\pi$ anomaly:

$$\frac{F_{3\pi}}{3} = \frac{1}{\pi}\int_{s_{\text{thr}}}^{\infty} ds' \frac{\operatorname{Im} a(s')}{s'}$$

Fit results $e^+e^- \to 3\pi$ cross section data

Parameters:

- resonance parameters M_ω, Γ_ω, M_ϕ, Γ_ϕ, c_ω, c_ϕ, $c_{\omega'}$, $c_{\omega''}$
- conformal parameters c_1, c_2, c_3
- energy rescaling $\sqrt{s} \to \sqrt{s} + \xi(\sqrt{s} - 3M_\pi)$
  $\longrightarrow$ far less an issue than for $\pi^+\pi^-$

Fit results $e^+e^- \to 3\pi$ cross section data

Parameters:

- resonance parameters $M_\omega,\ \Gamma_\omega,\ M_\phi,\ \Gamma_\phi,\ c_\omega,\ c_\phi,\ c_{\omega'},\ c_{\omega''}$
- conformal parameters $c_1,\ c_2,\ c_3$
- energy rescaling $\sqrt{s} \to \sqrt{s} + \xi(\sqrt{s} - 3M_\pi)$
  $\longrightarrow$ far less an issue than for $\pi^+\pi^-$
- quality of the combined fit to all data:

	this work		
χ^2/dof	430.8/305	=	1.41

▷ correlations increase χ^2/dof by $\sim$ 0.3

▷ significantly better fits to individual data sets
$\longrightarrow$ fit errors inflated by scale factor $S = \sqrt{\chi^2/\text{dof}}$

Fit results $e^+e^- \to 3\pi$: ω, ϕ peaks

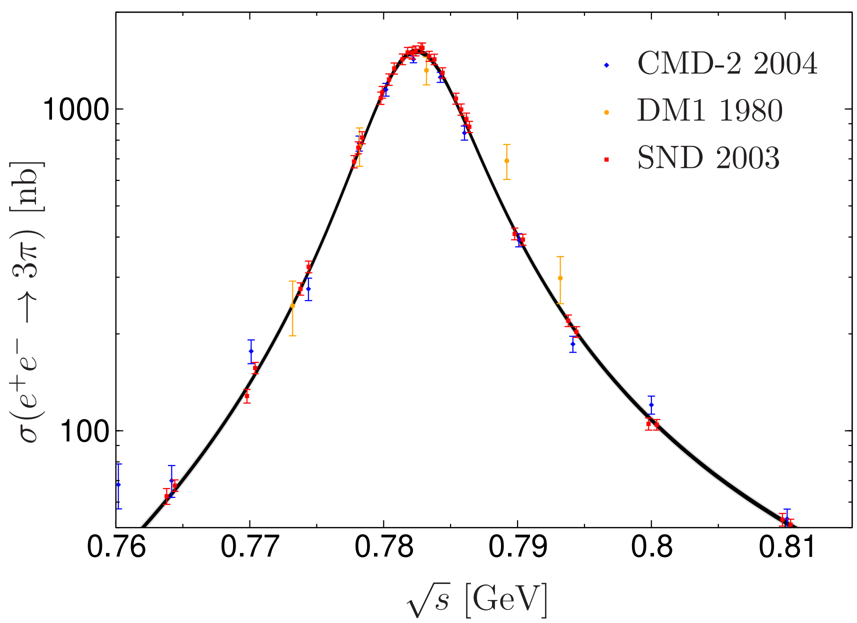

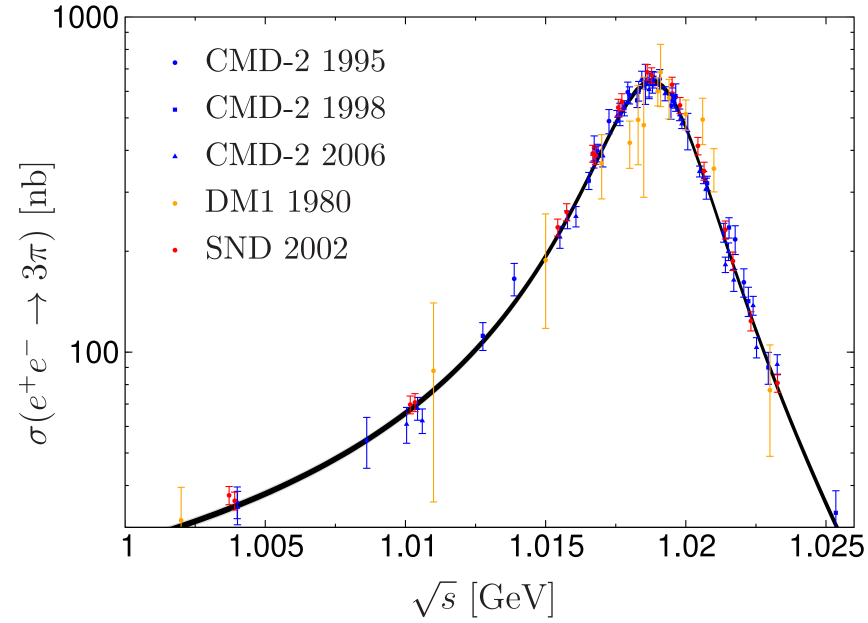

- VP-subtraction: expect $\Delta M_\omega = -0.13$ MeV, $\Delta M_\phi = -0.26$ MeV

$$M_\omega = 782.63(3)\ \text{MeV} \qquad \Gamma_\omega = 8.71(6)\ \text{MeV}$$
$$M_\phi = 1019.20(2)\ \text{MeV} \qquad \Gamma_\phi = 4.23(4)\ \text{MeV}$$

…vs. PDG:

$$M_\omega = 782.65(12)\ \text{MeV} \qquad \Gamma_\omega = 8.49(8)\ \text{MeV}$$
$$M_\phi = 1019.461(16)\ \text{MeV} \qquad \Gamma_\phi = 4.249(13)\ \text{MeV}$$

$\longrightarrow$ M_ω compatible with PDG [but tension with $\pi\pi$ (!) channel]

Fit to $\pi^0\gamma$ instead: HVP contribution

- fit disp. representation to $e^+e^- \to \pi^0\gamma$ instead of 3π data
  $\longrightarrow$ excellent consistency, average pole parameters:

	$e^+e^- \to 3\pi, \pi^0\gamma$	PDG
$\bar{M}_\omega$ [MeV]	$782.736(24)$	$782.65(12)$
$\bar{\Gamma}_\omega$ [MeV]	$8.63(5)$	$8.49(8)$
$\bar{M}_\phi$ [MeV]	$1019.457(20)$	$1019.461(16)$
$\bar{\Gamma}_\phi$ [MeV]	$4.22(5)$	$4.249(13)$

- $\pi^0\gamma$ HVP contribution: Hoid, Hoferichter, BK 2020

$$\boxed{a_\mu^{\pi^0\gamma}|_{\leq 1.35\,\mathrm{GeV}} = 43.8(6)(1) \times 10^{-11} = 43.8(6) \times 10^{-11}}$$

- good agreement (except small interpolation errors):

Davier et al. 2019	Keshavarzi et al. 2019
$44.1(1.0)$	$45.8(1.0)$

Summary: processes and unitarity relations for $\pi^0 \to \gamma^*\gamma^*$

process	unitarity relations	SC 1	SC 2
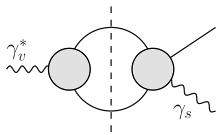	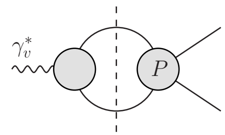		$F_{\pi^0\gamma\gamma}$
	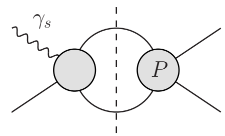	$F_{3\pi}$	$\sigma(\gamma\pi \to \pi\pi)$
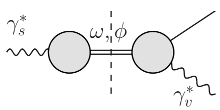	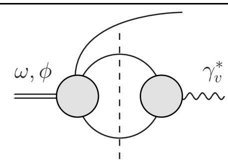		$\Gamma_{\pi^0\gamma}$
	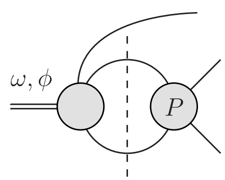	$\Gamma_{3\pi}$	$\frac{d^2\Gamma}{ds\,dt}(\omega,\phi \to 3\pi)$
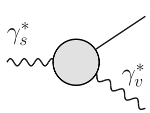	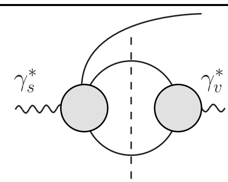		$\sigma(e^+e^- \to \pi^0\gamma)$
	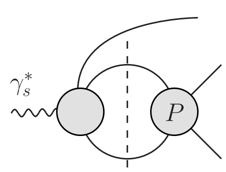	$\sigma(e^+e^- \to 3\pi)$	$\sigma(\gamma\pi \to \pi\pi)$ $\frac{d^2\Gamma}{ds\,dt}(\omega,\phi \to 3\pi)$
	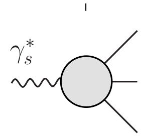	$F_{3\pi}$	$\sigma(e^+e^- \to 3\pi)$

Colangelo, Hoferichter, BK, Procura, Stoffer 2014

$\gamma\pi \to \pi\pi$

$\omega \to 3\pi$, $\phi \to 3\pi$

$\gamma^* \to 3\pi$

common theme:
resum $\pi\pi$ rescattering